Response to the referee comments on the manuscript:

Title: Developing and bounding ice particle mass- and area-dimension expressions for use in atmospheric models and remote sensing
By: Erfani, Ehsan; Mitchell, David
Article reference: acp-2015-739

We wish to thank the referees for their detailed and helpful comments on our paper. As you will see below we have responded to all of the comments with revisions designed to address the concerns of the referees. In the following response, the original referee comments appear in black and our responses appear in blue and are labeled "Author response:"

Referee comments:

Anonymous Referee #2:

Review on "Developing and bounding ice particle mass- and area-dimension expressions for use in atmospheric models and remote sensing" submitted to Atmospheric Chemistry and Physics by E. Erfani and D. L. Mitchell

The paper describes a level more complex and better fit to m-D and A-D relationships than the traditional power law relationships, and then the paper presents an accommodation on how the more complex relations can be used in climate and cloud models without requiring all too expensive computation.

The reviewer is especially impressed on the quality of the writing, and the thoroughness and completeness of the arguments. While we may have differences in writing style and different preferences for expressing error or representing measurements, the paper comes across as well edited and prepared. Also clearly the topic is relevant and makes an important line-item to list of potential improvements in climate modeling.

Recommendation is publication after revision addressing the following suggestions:

The reviewer's main concern in the paper in its current form is how the natural variability is represented, and how approximations are justified. The stated purpose of the paper is to "develop m-D and A-D expressions that are representative of all ice particles for a given cloud type and temperature interval, suitable for use in climate models." (28523/3-5) The goal is to get past the natural variation in ice crystal ensemble properties to an average parameterization suitable for representing ice crystal properties in _25x25kmˆ2 grid boxes in just _2 coefficients. Natural variation could be seen as a nuisance or unimportant noise. The reviewer would prefer to see it portrayed and dealt with more, while others might argue it's outside the scope of the paper. The reviewer argues that seeing the natural variation in figures and laid out more clearly in text strengthens the paper in that it helps the reader understand and trust the results more than if it goes un-portrayed and unsaid.

Author response: We added a "supplement" to the paper that contains a two-panel figure that shows m-D and A-D expressions and data points for all PSDs without the temperature dependence (Fig. S5). Also shown in this figure is mean and standard deviation in each size bin. In this way, the natural variability of m-D and A-D expressions is presented. This figure is now mentioned at the first paragraph of Sect. 3 along with the discussion on the variability of m-D expression. The natural variability associated with ice particle mass measurements was minimized in two ways. First, m was estimated from the BL2006 m-A relationship for $D > 200$ μm (which represents the mean m-A behavior in a self-consistent way and thus removes much of the natural variability in m), and second, variability was reduced by averaging the SPARTICUS PSD within each 5 °C T interval, as described in Sect. 2, producing one mean PSD of number, area and mass concentration for each T interval.

We also added more discussions: McFarquhar et al. (2007) showed that there is considerable variability in m-D expression during the aircraft measurements of stratiform regions of mesoscale convective systems, and they used different m-D expression for each flight. However, as we show further in this section, the standard deviation in m-D relationship based on 13 flights in synoptic cirrus clouds during SPARTICUS does not exceed 32 % of the mean bin mass value, having a mean overall value of 13.48 %.

Now, the first paragraph in Sect. 3 has changed (original manuscript, page 28527, starting at line 16):

"Figure S5 shows m-D and A-D expressions and data points for all PSDs for all temperatures considered here. Also shown in this figure is mean and standard deviation in each size bin. In this way, the natural variability of the m-D and A-D PSD data is presented. While in principle each PSD can be used to produce an m-D or A-D expression, in practice only the mean PSDs in 5 °C temperature intervals were used to develop the m-D and A-D expressions (explained in Sect. 2.3 and in the Supplement, Fig. S6). Although the averaging process reduces scatter, the coherency of the curves in Fig. S6 is somewhat surprising. The natural variability associated with ice particle mass measurements was minimized in two ways, thus facilitating the curve-fitting process. First, m was estimated from the BL2006 m-A relationship for $D > 200$ μm (which represents the mean m-A behavior in a self-consistent way and thus removes much of the natural variability in m), and second, variability was reduced by averaging the SPARTICUS PSD within each 5 °C T interval, as described in Sect. 2, producing one mean PSD of number, area and mass concentration for each T interval. The latter can be seen by comparing Figs. S5 and S6. The coherency of this data makes it amenable to curve-fitting with high precision. McFarquhar et al. (2007) showed that there is considerable variability in the m-D expression during aircraft measurements of stratiform regions of mesoscale convective systems, and they used different m-D expression for each flight. However, as we show further in this section, the variability in m-D relationship based on 13 flights in synoptic cirrus clouds during SPARTICUS does not exceed 32 % of the mean bin mass value, having a mean overall value of 13.48 %."

And we added a sentence (original manuscript, page 28523, line 5) and referred the reader to Sec. 3 for the discussion on variability:

"… (see Sect. 3 for the discussion of variability in *m-D* and *A-D* expressions)."

28527/18, Suggested is a two-panel figure showing something similar to Figure 5, but with data points from each temperature range in Tables 1 and 2 on m-D and A-D axes. The idea being to show the scatter.

Author response: A two-panel figure is added that shows A-D and m-D data points averaged for PSDs in 5 °C temperature intervals (Fig. S6). This is actually the figure that was not shown in the original manuscript, but was explained in this part. To avoid the repetitive explanations, we refer to the previous comment immediately above. The manuscript has also been modified to refer to this figure (original manuscript, page 28527, starting at line 16) as described in the previous comment.

28528/19, Says greater accuracy can be made by fitting to temperature intervals. But the fits appear so similar in Figure 4. Could the authors please comment on a fit without the temperature dependence, and quantify the improvement in splitting up into temperature regimes? How could a climate model smoothly vary between the fits once a temperature boundary is crossed?

Author response: We agree that the fits in Fig. 4 are similar, and the regression equations for the A-D and m-D plots in Fig. S5, based on all temperatures, are now included for those who would prefer temperature-independent relationships. While the R^2 for these curve fits (0.9924 and 0.9954, respectively) is similar to those in Tables 1 and 2, the actual values predicted by the three temperature-dependent fits does render more accurate A and m estimates, as shown in Figs. 4 and S6. Qualitative improvements in accuracy can be estimated from the figures while quantitative improvements can be calculated via Tables 1 and 2. Since indeed the fits are similar, a climate model can use these fits without using any smoothing function when crossing temperature boundaries. In fact, this m-D/A-D scheme has already been used in CAM5, as described in Eidhammer et al. (2016, submitted to J. Climate).

These explanations have been added to manuscript (original manuscript, page 28528, starting at line 21):

"…While the temperature-dependent A-D and m-D fits are similar, and the R^2 values for the temperature-independent A-D and m-D fits in Fig. S5 (0.9924 and 0.9954, respectively, based on all temperatures) are similar to those in Tables 1 and 2, the actual values predicted by these temperature-dependent fits does render more accurate A and m estimates, as shown in Figs. 4 and S6. Since the fits are similar, a climate model can use these fits without using any smoothing function when crossing temperature boundaries. In fact, this m-D/A-D scheme has been used in a GCM, as described in Eidhammer et al. (2016). …"

28524/26-30, The "all-in“ criteria limits the sample volume for the larger ice crystals measured by the 2D-S. That is, a 1mm ice crystal has a smaller chance of appearing all-in vs. a 0.2 mm crystal. If this limitation in volume sample rate is accounted for, it should be stated.

Author response: We added a supplement document that has been provided by SPEC Inc. to compare the M1 and M7 methods, and it addresses this issue. Although the sample volume decreases by using the M7 method, such a decrease is not considerable. Figures S1 and S3 show number concentration and area concentration as functions of maximum dimension for cases of synoptic and anvil cirrus clouds, respectively. It is seen that the M1 and M7 methods agree well for both number concentration and area concentration, and the larger difference between the M1 and M7 methods is observed for larger particles (D > 300 μm). Moreover, the comparison of the M1 and M7 methods for the PSD number concentration and extinction is displayed in Figs. S2 and S4. The difference in sample area between M1 and M7 methods does not exceed 5 % and 13 % for synoptic and anvil cirrus clouds, respectively. In other words, the difference for projected area is more pronounced in anvil than in synoptic cirrus clouds due to the existence of slightly larger ice particles in anvil clouds that have a greater chance of intersecting the edges of the 2D-S field of view. This explanation is added to the text (original manuscript, page 28524, starting at line 29):

"… Although the sample volume decreases by using the M7 method, such a decrease is not significant. It is shown in the supplement (Figs S1 and S2) that the M1 and M7 methods agree well for both number concentration and area concentration, with the largest difference between the M1 and M7 methods observed for larger particles (D > 300 μm). Moreover, the difference in PSD projected area (i.e. extinction) between the M1 and M7 methods does not exceed 5 % and 13 % for synoptic and anvil cirrus clouds, respectively (see Appendix A for detailed discussion on the comparison between M1 and M7 methods). …"

And Appendix A has been modified (original manuscript, page 28544, starting at line 8):

"…Although the sample volume decreases by using M7 method, such a decrease is not significant. Figures S1 and S3 show number concentration and area concentration as functions of maximum dimension for cases of synoptic and anvil cirrus clouds, respectively. It is seen that the M1 and M7 methods agree well for both number concentration and area concentration, with a larger difference between the M1 and M7 methods observed for larger particles (D > 300 μm). Moreover, the comparison of the M1 and M7 methods for the PSD number concentration and extinction is displayed in Figs. S2 and S4. The difference in PSD projected area (i.e. extinction) between the M1 and M7 methods does not exceed 5 % and 13 % for synoptic and anvil cirrus clouds, respectively. Such difference in projected area is more pronounced in anvil than in synoptic cirrus due to slightly larger ice particles in anvil clouds that have a greater chance of intersecting the edges of the 2D-S field of view. "

28543/10-13, The reviewer invites the authors to speculate on how broadly this fit might be applied to other similar clouds such as tropical or subtropical anvil cirrus, or perhaps arctic cirrus. The fact is many parameterization studies such as Brown and Francis 1996 are applied (extrapolated) outside their valid regime in models and other studies (Heymsfield et al. 2010). The synoptic and anvil cloud fits in this paper aren't so different. How different could the fits to ice particle data

from other clouds be? Or where might the ice appear so different these parameterizations would be clearly inappropriate to use? Any insight would be appreciated.

Author response: A study by Lawson (2016) has recently been conducted to address this exact question, as the BL2006 m-A power law has been demonstrated to not work well for Arctic clouds. Therefore a similar m-A study was conducted but this time using planar ice crystals having relatively low aspect ratios (<< 1). Citing this study, we have added a new paragraph to Section 3 (shown below) to address this important question:

If ice particle morphology does not vary much within the cirrus clouds sampled, then our *m-D* expressions should be representative of all ice particles for a given cloud type (continental midlatitude synoptic or anvil cirrus clouds) and temperature interval. Ice particle images from various types of cirrus clouds tend to support this assumption, indicating high density, blocky-shaped irregular crystals with some bullet rosettes and side planes at larger sizes (e.g. Lawson et al., 2006b; Baker and Lawson, 2006b). But if there is a radical departure from this morphology genre and planar ice crystals having low aspect ratios (i.e. c-axis to a-axis ratio where c-axis is length of the prism face) dominate, our m-D expressions could overestimate ice particle mass by a factor of ~ 3 (Lawson, 2016). Such reasoning may explain findings from Arctic mixed phase clouds, where Jackson et al. (2012) showed that the application of habit-specific *m-D* relationships applied to size/shape distributions in arctic stratocumulus clouds during Indirect and Semi-Direct Aerosol Campaign (ISDAC) over North Slope of Alaska had better agreement with the measured IWC (mean difference is ~ 50%) than did the application of the BL2006 approach to the measured size distributions (mean difference is ~ 100%). Similar findings from Arctic mixed phase clouds are reported in Avramov et al. (2011).

The manuscript has been modified to reflect all these changes (original manuscript, page 28528, before line 1):

"If ice particle morphology does not vary much within the ice clouds sampled, then our *m-D* expressions should be representative of all ice particles for a given cloud type (continental midlatitude synoptic or anvil cirrus clouds) and temperature interval. Ice particle images from various types of cirrus clouds tend to support this assumption, indicating high density, blocky-shaped irregular crystals with some bullet rosettes and side planes at larger sizes (e.g. Lawson et al., 2006b; Baker and Lawson, 2006b). But if there is a radical departure from this morphology genre and planar ice crystals having low aspect ratios (i.e. c-axis to a-axis ratio where c-axis is length of the prism face) dominate, our m-D expressions could overestimate ice particle mass by a factor of ~ 3 (Lawson, 2016). Such reasoning may explain findings from Arctic mixed phase clouds, where Jackson et al. (2012) showed that the application of habit-specific *m-D* relationships applied to size/shape distributions in arctic stratocumulus clouds during Indirect and Semi-Direct Aerosol Campaign (ISDAC) over North Slope of Alaska had better agreement with the measured IWC (mean difference is ~ 50%) than did the application of the BL2006 approach to the measured size distributions (mean difference is ~ 100%). Similar findings from Arctic mixed phase clouds are reported in Avramov et al. (2011)."

The manuscript has also been modified to address the Conclusions (original manuscript, page 28543, starting at line 10):

"This study was focused only on mid-latitude continental ice clouds, and not on marine anvil or synoptic cirrus, orographic cirrus and/or Arctic ice clouds. Application of BL2006 (which is based

on a subset of SCPP data from mid-latitude continental clouds) to tropical anvil clouds produced IWC with only ~ 18% difference compared to measured bulk IWC (Lawson et al. 2010). However, use of BL2006 in artic mixed phase clouds leads to IWC ~ 100% larger than measured bulk IWC (Jackson et al. 2012). Additional research is required to apply and test the approach introduced in this study in different environments."

28544/21-22, The reviewer invites the authors to quantify in some way how much their columnar representation of small ice crystals is more accurate than the traditional spherical ice assumption.

Author response: We thank the reviewer for this suggestion; An explanation has been added to the end of Appendix B (original manuscript, page 28546, after line 18):

"One benefit of the hexagonal column assumption is consideration of ice particle aspect ratio. The spherical ice assumption means that the aspect ratio is unity. Assuming that ice particles are spherical, their mass can be calculated as a function of projected area (e.g. $m_{sphere} = \rho_i \frac{4}{3\sqrt{\pi}} A_{sphere}^{3/2}$). We calculated the percent difference of mass between the spherical and hexagonal column assumptions (where column aspect ratio = 1.0), and this value is ~ 4%."

This issue was brought up by the other referee, and this point is now addressed in the text (original manuscript, page 28526, starting at line 25):

"This new methodology assumes that ice particles with size less than 100 μm exhibit hexagonal column geometry. Such a geometrical assumption seems reasonable based on observations for sizes smaller than 100 μm (see Lawson et al., 2006, their Figs. 4 and 5). While other authors have approximated small (e.g. D < 50 μm) ice crystals as "droxtals", Gaussian random spheres, Chebyshev particles and budding bucky balls (e.g. Um and McFarquhar, 2009), our study estimates the mass of small ice particles from processed CPI data that contains measurements of ice particle projected area, length and width. We developed a method that utilizes all three of these properties to estimate ice particle mass. For the size-range we considered (20 to 100 μm), the mean length-to-width ratio was 1.41±0.26, confirming the dominance of high-density ice particles, and for such aspect ratios, hexagonal columns appear to be as good a surrogate of small particle morphology as the other shapes noted above for estimating ice particle mass. They also provide a convenient means of using the aspect ratio estimates. As shown in Appendix B, for an aspect ratio of 1.0, the difference in ice mass between the spherical and hexagonal column assumption is 4%. "

Tables 1 and 2, How were the temperature ranges -40 to -20, -55 to -40, and -65 to -55 chosen, with their uneven intervals? Was there a similarity criteria that led to putting the 5C temperature intervals together sometimes, and not other times?

Author response: First, we calculated values of mean dimension, mass, and projected area for each 5 °C T interval, and provided plots of m-D and A-D expressions for each 5 °C T interval. We then observed that m-D and A-D expressions for 5 °C T intervals have negligible differences within the larger temperature ranges of -40 °C < T < -20 °C, -55 °C < T < -40 °C, and -65 °C < T < -55 °C. In order to keep m-D and A-D expressions as simple as possible without losing accuracy, we did not provide Tables 1 and 2 for each 5 °C T interval. However for uncertainty calculations, we kept

the 5 °C T interval, because such similarity criteria is not observed for uncertainty and variability. This explanation has been added to the manuscript (original manuscript, page 28528, starting at line 16):

"Values of mean dimension, mass, and projected area were first calculated for each 5 °C *T* interval, and plots of *m*-*D* and *A*-*D* expressions were provided for each 5 °C *T* interval (Fig. S6). It was then observed that *m*-*D* and *A*-*D* expressions for 5 °C *T* intervals have negligible differences within the larger temperature ranges of -40 °C < *T* < -20 °C, -55 °C < *T* < -40 °C, and -65 °C < *T* < -55 °C. In order to keep *m*-*D* and *A*-*D* expressions as simple as possible without losing accuracy, the coefficients of polynomial fits are not provided for each 5 °C *T* interval. Instead, the mean PSDs were grouped into the above mentioned three temperature categories and 2nd order polynomial curve fits were calculated for each category as shown in Tables 1 and 2. …"

Figure A1 lacks orientation for the reader. Suggested is adding axes to show flow direction, diode array direction and diode array width. Why are there two ice particle shadowgraphs shown? What's the difference between them? Why is L4 in the right figure so much smaller than its crystal?

Author response: All the orientations and directions (e.g. axes, flow direction, photodiode array direction and width) have been added to Figure A1. Two ice particles are shown to give the reader an idea of how different length scales (L1, L4, and MaxLength) for different ice particle shapes are measured and calculated by 2D-S and its respective software. L4 is not the particle "height" range (projected along the vertical photodiode array) during its entire transit time through the sample volume; rather it is a measure of particle width at a given instant. Moreover, L4 is the maximum value of all these time-slices or widths measured. This latter point may be better illustrated by the ice particle on the left. This clarification about L4 has been added to Appendix A (original manuscript, page 28543, starting at line 25):

"… Note that length scale L4 in Fig. A1 is not the particle "height" range (projected along the vertical photodiode array) during its entire transit time through the sample volume; rather it is a measure of particle width at a given instant. Moreover, L4 is the maximum value of all these time-slices (i.e. widths) measured."

Also added to Appendix A is the clarification of two ice particles with different shapes (original manuscript, page 28543, starting at line 18):

"…First, the M1 and M7 methods differ on the measurement of particle dimensions, as is shown in Fig. A1. Two ice particles with different shapes are shown to give the reader an idea of how the different length scales (L1, L4, and MaxLength) for different ice particle shapes are measured and calculated by the 2D-S and its respective software. …"

Figure B1 and the discussion in Appendix B1 on planes P1, P2 and P3. The reviewer is at a complete loss how these planes and the columnar crystal in the CPI sample volume are oriented. By far the best help would be a helpful drawing or figure. Suggested is adding orientation information to Figure B1. Show the axes, the planes, and the instrument sample volume.

Author response: The axes, planes, flow direction and photodiode array have been added to Figure B1. Also provided is 3 extra panels that show how the hexagonal column is projected, when its c-axis is parallel to P1, P2, or P3. Figure B1 caption has been modified to:

"Figure B1. a) 3-D geometry of a hexagonal prism, representative of small ice crystals. Assuming that the direction of view (beam direction) is along the x-axis, P1 is orthogonal to x-axis, P2 is orthogonal to y-axis, and P3 is orthogonal to z axis. Also shown is the projection of a hexagonal prism for three extremes, when its c-axis is parallel to b) P1, c) P2, and d) P3. See text for the definition of various symbols."

28528/21 resulted -> resulting

Author response: "resulted" has been changed to "resulting".

28545/16 Formula should be 3ˆ(3/2) aˆ2 / 8, if the reviewer understands the variable meaning correctly

Author response: Thank you for noticing to this typo. We corrected this, and checked other derivations. All other calculations were correct.

The paper has just enough symbols, it may be appropriate to add a variable index.

Author response: We added the list of variables as Appendix C (original manuscript, page 28547, starting at line 8):

"Appendix C: List of symbols

a	maximum dimension across the basal face of a hexagonal crystal
a_v	prefactor in fall speed-dimension power law
A	projected area
$\langle A \rangle$	average projected area of a hexagonal crystal for all orientations
$A_{b,\max}$	area of the basal face of a hexagonal crystal
$A_{p,\max}$	area of the prism face of a hexagonal crystal
A_r	area ratio
A_t	total PSD projected area
b_v	exponent in fall speed-dimension power law
c	length along the prism face of a hexagonal crystal
D	maximum dimension of ice particle
D_o	characteristic dimension of the ice PSD
$\overline{D}$	mean maximum dimension of a PSD
D_A	median area dimension

D_e	effective diameter
D_i	dimension of interest
D_m	median mass dimension
D_N	number concentration dimension
D_Z	reflectivity dimension
g	gravitational constant
IWC	ice water content
m	mass of ice particle
N	number concentration
N_o	prefactor of a gamma PSD
PSD	particle size distribution
R	relative ratio of mass to area
R^2	coefficient of determination
T	temperature
V	terminal fall speed of ice particle
V_h	volume of a hexagonal crystal
V_m	mass-weighted terminal fall speed
Z	radar reflectivity
X	Best number
α	prefactor in mass-dimension power law
β	exponent in mass-dimension power law
γ	prefactor in projected area-dimension power law
δ	exponent in projected area-dimension power law
Γ	gamma function
ε	apparent aspect ratio
ζ	true aspect ratio
η	dynamic viscosity of air
λ	slope parameter of a gamma PSD
ν	dispersion parameter of a gamma PSD
σ	standard deviation
ρ_{air}	density of air
ρ_i	bulk density of ice”

Added References:

Avramov, A., and co-authors: Toward ice formation closure in Arctic mixed-phase boundary layer clouds during ISDAC, J. Geophys. Res.-Atmos., 116, D00T08, doi:10.1029/2011JD015910, 2011.

Baker, B. A., and Lawson, R. P.: In Situ Observations of the Microphysical Properties of Wave, Cirrus, and Anvil Clouds. Part I: Wave Clouds, J. Atmos. Sci., 63, 3160-3185, 2006b.

Eidhammer, T., Morrison, H., Mitchell, D. L., Gettelman, A., and Erfani, E.: Improvements in

the Community Atmosphere Model (CAM5) microphysics using a consistent representation of ice particle properties. Submitted to J. Climate in Dec., 2015.

Fontaine, E., Schwarzenboeck, A., Delanoe, J., Wobrock, W., Leroy, D., Dupuy, R., Gourbeyre, C., and Protat, A.: Constraining mass-diameter relations from hydrometeor images and cloud radar reflectivities in tropical continental and oceanic convective anvils, Atmos. Chem. Phys., 14, 11367-11392, doi:10.5194/acp-14-11367-2014, 2014.

Jackson, R. C., McFarquhar, G. M., Korolev, A. V., Earle, M. E., Liu, P. S., Lawson, R. P., Brooks, S., Wolde, M., Laskin, A., and Freer, M.: The dependence of ice microphysics on aerosol concentration in arctic mixed-phase stratus clouds during ISDAC and M-PACE, J. Geophys. Res. -Atmos., 117, doi:10.1029/2012JD017668, 2012.

Jensen, E. J., Lawson, R. P., Bergman, J. W., Pfister, L., Bui, T. P., and Schmitt, C. G.: Physical processes controlling ice concentrations in synoptically forced, midlatitude cirrus, J. Geophys. Res.-Atmos., 118, 5348-5360, doi:10.1002/jgrd.50421, 2013.

Lawson, R. P., B. A. Baker, B. A., Pilson, B., and Mo, Q.: In situ observations of the microphysical properties of wave, cirrus and anvil clouds. Part II: Cirrus clouds. J. Atmos. Sci., 63**,** 3186–3203, 2006b.

Lawson, R. P.: Improvement in Determination of Ice Water Content from Two-Dimensional Particle Imagery. Part III: Ice Particles with High a- to c-axis Ratio. Submitted to J. Appl. Meteorol. and Climate, 2016.

Locatelli, J. d., and Hobbs, P. V.: Fall speeds and masses of solid precipitation particles, J. Geophys. Res., 79, 2185-2197, doi:10.1029/JC079i015p02185, 1974.

McFarquhar, G. M., Timlin, M. S., Rauber, R. M., Jewett, B. F., and Grim, J. A.: Vertical variability of cloud hydrometeors in the stratiform region of mesoscale convective systems and bow echoes, Mon. Wea. Rev., 135, 3405-3428, doi:10.1175/mwr3444.1, 2007.

McFarquhar, G. M., Um, J., and Jackson, R.: Small Cloud Particle Shapes in Mixed-Phase Clouds, J. Appl. Meteor. Climatol., 52, 1277–1293, doi: http://dx.doi.org/10.1175/JAMC-D-12-0114.1, 2013

Um, J., and McFarquhar, G. M.: Dependence of the single-scattering properties of small ice crystals on idealized shape models, Atmos. Chem. Phys., 11, 3159-3171, doi:10.5194/acp-11-3159-2011, 2011.

Modified Figures:

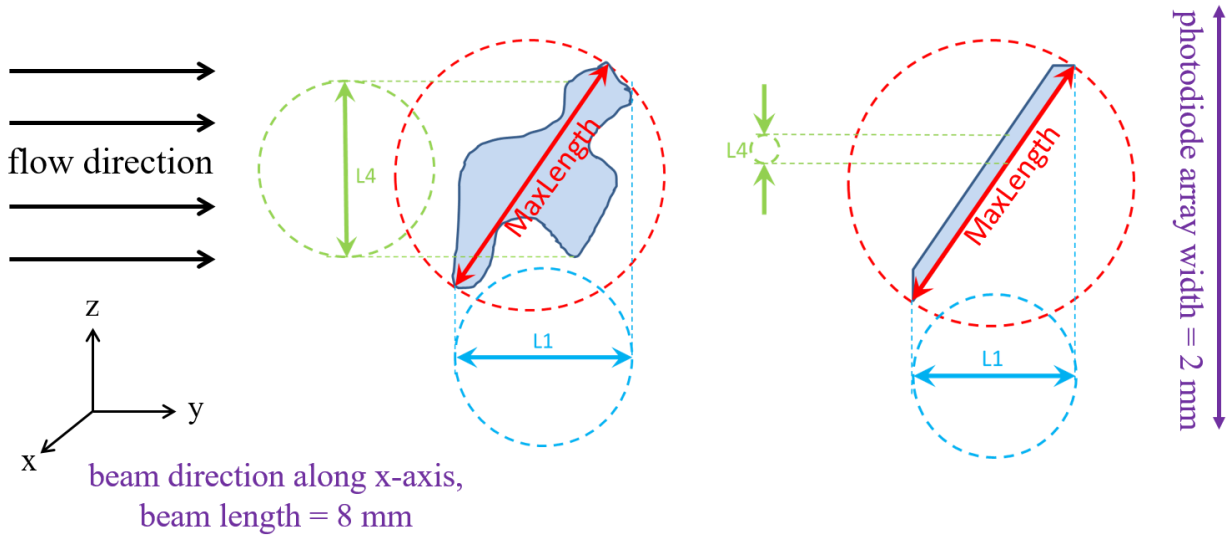

Figure A1. Geometry of dimension measurements showing length scales for the M1 method (*L1*) and the M7 method (MaxLength) for two ice particles with different shapes. Courtesy of Paul Lawson and Sara Lance.

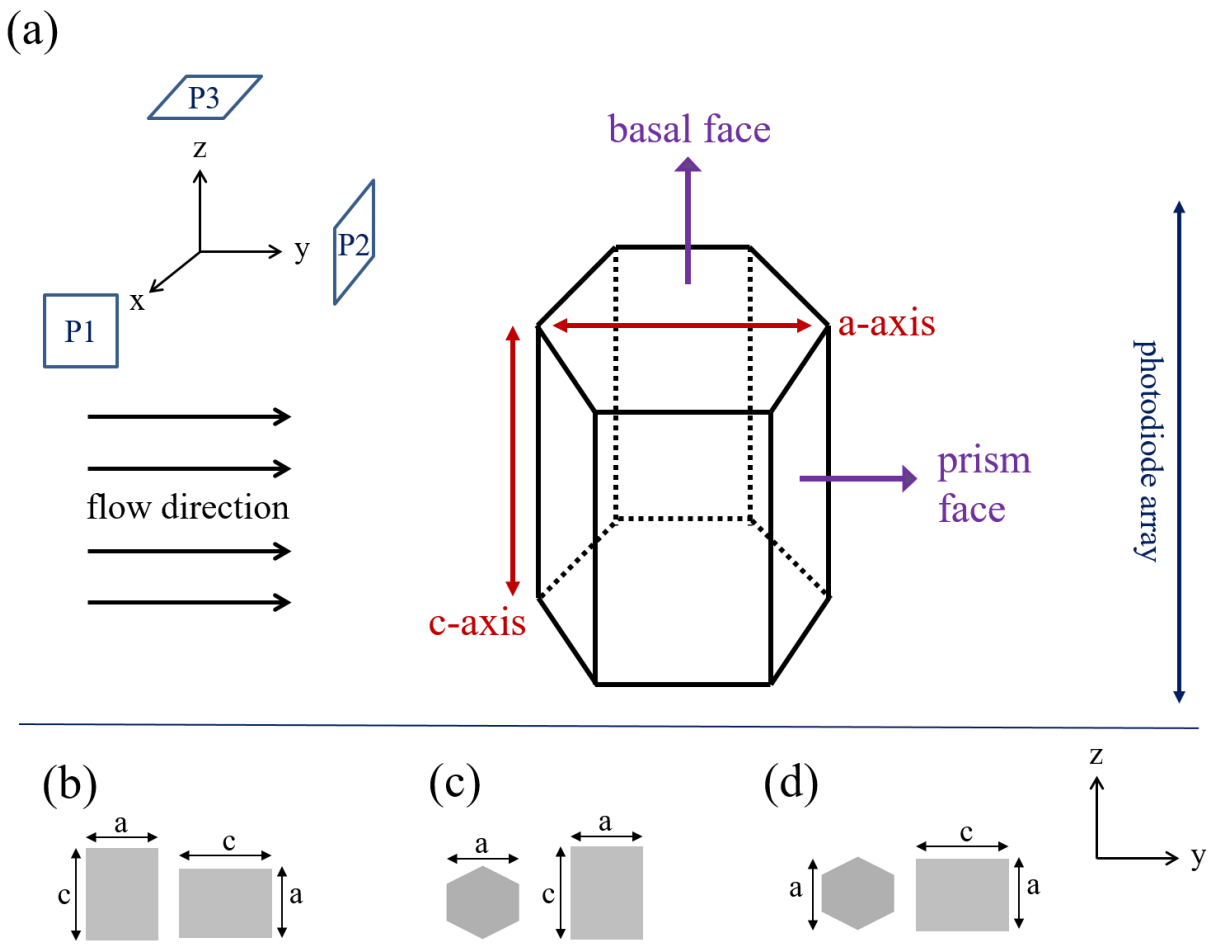

Figure B1. a) 3-D geometry of a hexagonal prism, representative of small ice crystals. Assuming that the direction of view (beam direction) is along the x axis, P1 is orthogonal to x axis, P2 is orthogonal to y axis, and P3 is orthogonal to z axis. Also shown is the projection of a hexagonal prism for three extremes, when its c-axis is parallel to b) P1, c) P2, and d) P3. See text for the definition of various symbols.

Supplement:

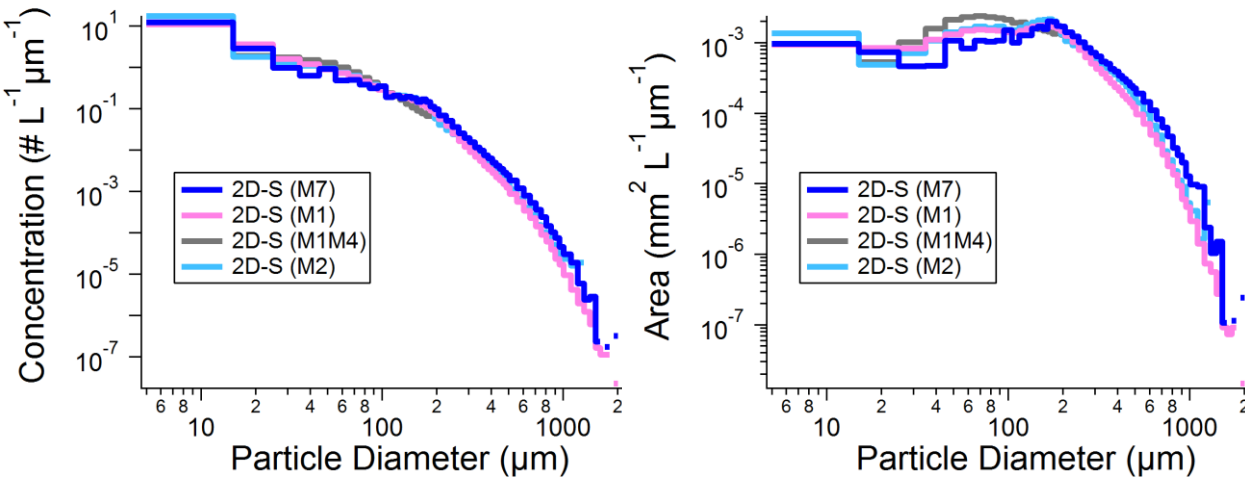

(a) (b)

Figure S1. (a) Ice particle number concentration and (b) ice particle projected area concentration as functions of maximum dimension for various processing method of 2D-S data during flight A on 19 Jan. 2010 (as example of synoptic cirrus clouds). Courtesy of Paul Lawson and Sara Lance.

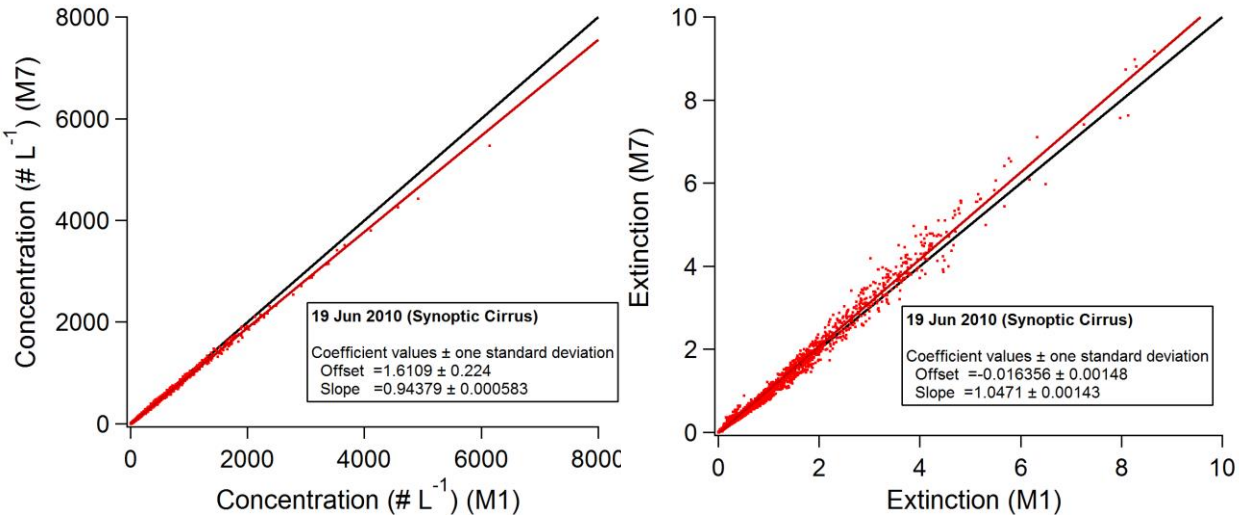

(a) (b)

Figure S2. (a) PSD number concentration from 2D-S M7 versus PSD number concentration from 2D-S M1, (b) extinction from 2D-S M7 versus extinction from 2D-S M1 during flight A on 19 Jan. 2010 (as example of synoptic cirrus clouds). Red line shows regression line to the data points, and black line displays 1:1 line. Courtesy of Paul Lawson and Sara Lance.

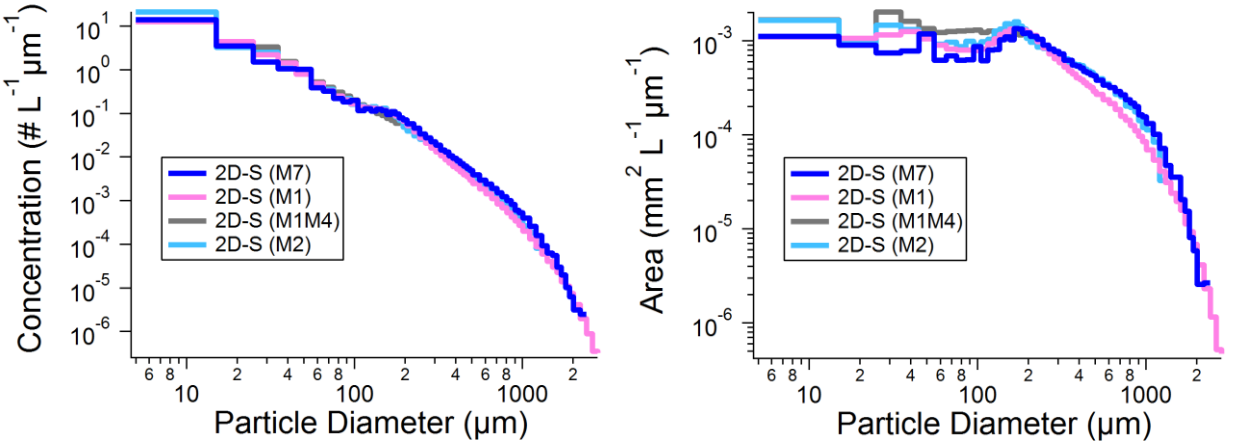

(a) (b)

Figure S3. Same as Fig. S1, but during flight A on 22 Apr. 2010 (as example of anvil cirrus clouds). Courtesy of Paul Lawson and Sara Lance.

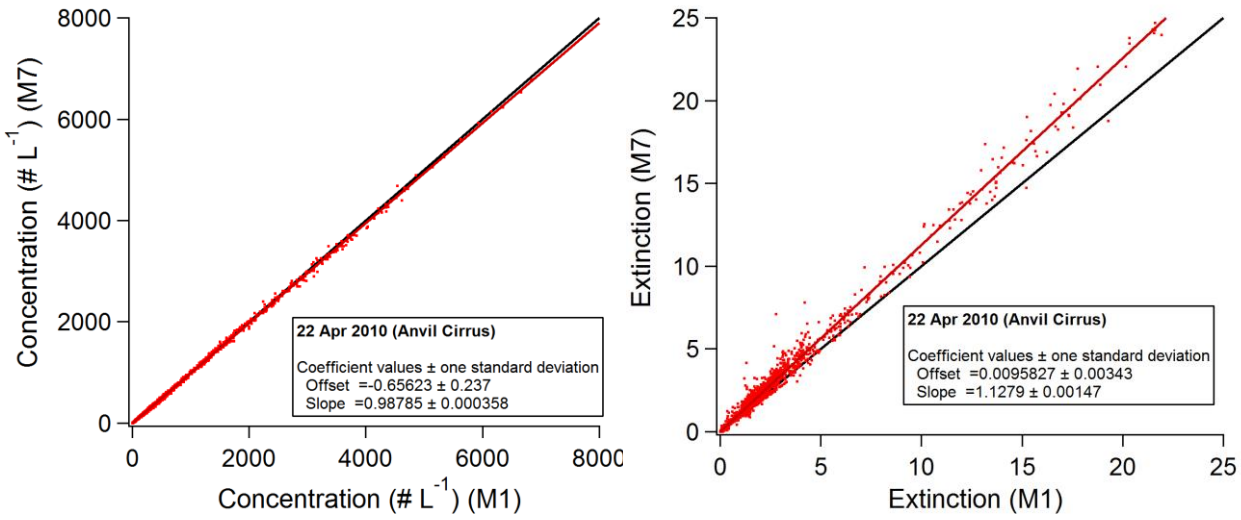

(a) (b)

Figure S4. Same as Fig. S2, but during flight A on 22 Apr. 2010 (as example of anvil cirrus clouds). Courtesy of Paul Lawson and Sara Lance.

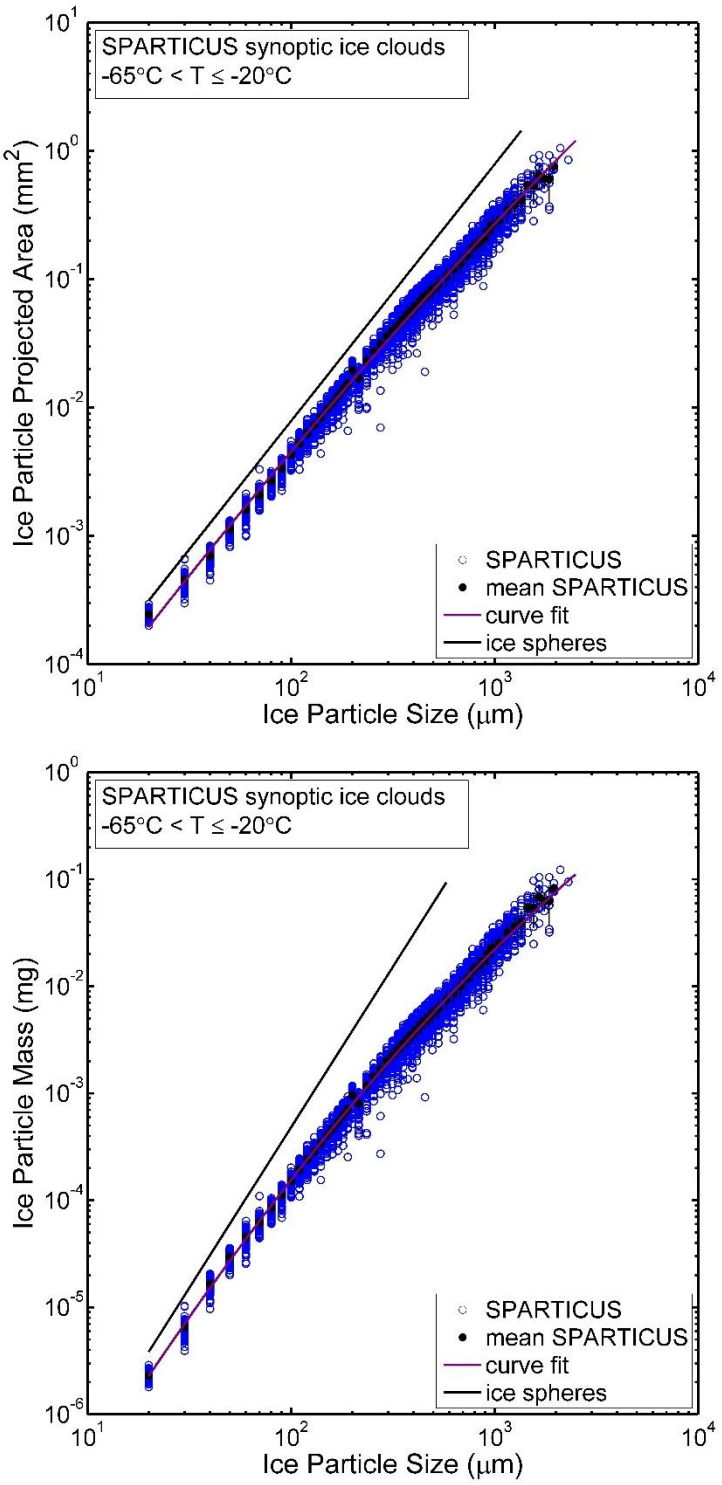

Figure S5. Dependence of (a) ice particle projected area and (b) ice particle mass on *D* based on actual PSDs regardless of temperature dependency. The SPARTICUS 2D-S data has been grouped into size-bins.

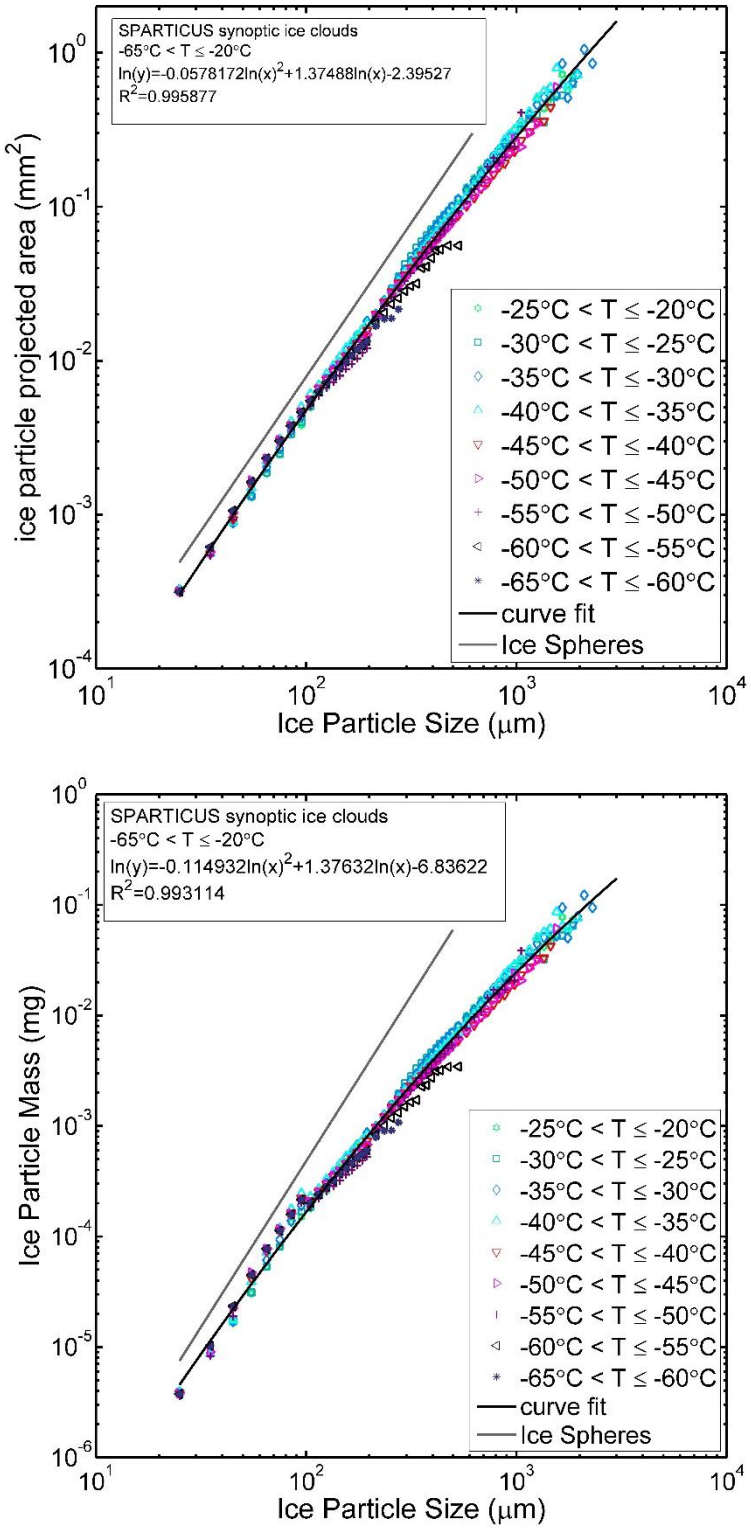

Figure S6. Dependence of (a) ice particle projected area and (b) ice particle mass on D based on mean PSD within the indicated temperature regime. The CPI and 2D-S data have been grouped into size-bins and 5 °C temperature intervals, and the black solid curve is a fit to these datasets.